bnhcrc.com.au

bushfire&natural HAZARDSCRC

THERMODYNAMIC CONSIDERATIONS OF PYROCUMULUS FORMATION

Peer reviewed research proceedings from the Bushfire and Natural Hazards CRC & AFAC conference
Sydney, 4 – 6 September 2017

K. Tory, W. Thurston and J. Kepert
Bureau of Meteorology, Research and Development
Bushfire and Natural Hazards CRC

Corresponding author: k.tory@bom.gov.au

Version	Release history	Date
1.0	Initial release of document	04/09/2017

Publisher:
Bushfire and Natural Hazards CRC

September 2017

Citation: Tory, K., Thruston, W. & Kepert, J. (2017). Thermodynamic considerations of pyrocumulus formation. In M. Rumsewicz (Ed.), Research forum 2017: proceedings from the research forum at the Bushfire and Natural Hazards CRC & AFAC Conference. Melbourne: Bushfire and Natural Hazards CRC.

Cover: Pyrocumulonimbus cloud formed above the Waroona fire, 7 January 2016. Image courtesy Tracy Vo Ch9 Perth

TABLE OF CONTENTS

ABSTRACT

In favourable atmospheric conditions, large hot fires can produce pyrocumulonimbus (pyroCb) cloud in the form of deep convective columns resembling conventional thunderstorms, which may be accompanied by strong inflow, dangerous downbursts and lightning strikes. These in turn may enhance fire spread rates and fire intensity, cause sudden changes in fire spread direction, and the lightning may ignite additional fires. Dangerous pyroCb conditions are not well understood and are very difficult to forecast.

Here, a conceptual study of the thermodynamics of fire plumes is presented to better understand the influence of a range of factors on plume condensation. Recognising that plume gases are undilute at the fire source and approach 100% dilution at the plume top (neutral buoyancy), we consider how the plume condensation height changes for this full range of dilution and for a given set of factors that include: environmental temperature and humidity, fire temperature, and fire moisture to heat ratios. The condensation heights are calculated and plotted as saturation point (SP) curves on thermodynamic diagrams for a broad range of each factor. The distribution of SP curves on thermodynamic diagrams provides useful insight into pyroCb behaviour. Adding plume temperature traces from Large-Eddy Model simulations to the thermodynamic diagrams provides additional insight into plume buoyancy, how it varies with height, and the potential for dangerous pyroCb development.

INTRODUCTION

Pyrocumulus (pyroCu) clouds are produced by heating of air from fire or volcanic activity that leads to ascent and subsequent condensation when the rising air becomes saturated due to cooling from adiabatic expansion. The process is similar to conventional convective cloud formation, when a lifting mechanism (e.g., orographic lifting, intersection of two air masses) raises air above the level at which cloud forms (the lifting condensation level). Additional lifting and condensational heating may raise the air to the level of free convection, above which it is positively buoyant. Turbulent entrainment of cooler and drier air from outside the rising airmass dilutes the cloud buoyancy, which can limit the size and growth of the cloud (e.g., fair weather cumulus). Larger and more intense lifted regions can accelerate to the tropopause (e.g., cumulonimbus thunderstorms). The main difference between conventional cumulus and cumulonimbus and fire-sourced pyroCu and pyroCb (hereafter referred collectively as pyroCu/Cb) clouds is that the initial lifting in the latter cloud types is provided by the buoyancy from the heat and perhaps moisture released by the fire. In large fires with an intense convection column the cloud may resemble towering cumulonimbus with updrafts that penetrate into the stratosphere (e.g., Fromm et al. 2010). We refer to these plumes as pyroCb. (See Tory et al 2015, 2016 for a review of pyroCu/Cb literature and forecast techniques respectively).

There is abundant evidence to suggest that the presence of pyroCb activity can have a significant impact on fire behaviour, including: (i) the amplification of burn- and spread-rates (Fromm et al. 2006, Trentmann et al. 2006, Rosenfeld et al. 2007, Fromm et al. 2012), (ii) enhanced spotting due to larger, taller and more intense plumes (e.g., Koo et al. 2010), and (iii) ignition of new fires by pyroCb lightning strikes due to pyroCb conditions favouring hotter and longer-lived lightning strikes (e.g., Rudlosky and Fuelberg 2011, Peace et al. 2017).

Given the potential threat posed by pyroCb there is great interest in being able to predict its development. Unfortunately, pyroCb are very difficult to forecast. Current forecast techniques draw on similarities between pyroCb and conventional thunderstorms, and the recognition that conditions that favour thunderstorm development will also favour pyroCb development (e.g., Peterson et al. 2015, Lareau and Clements 2016, Peterson et al. 2017). Ideal pyroCb conditions are thus similar to ideal thunderstorm conditions but with a dry rather than moist boundary layer. These conditions appear on a thermodynamic diagram as the classic inverted-V profile (e.g., Fig. 1), in which a dry adiabatic temperature profile of constant potential temperature (θ_{env}) forms the right side of the inverted-V, while the constant specific humidity (q_{env}) moisture profile makes up the left side.

In this paper we construct an idealized theoretical plume model in an inverted-V environment to aid our understanding of how the environment and fire properties influence plume condensation levels, which is important for understanding pyroCu/Cb formation.

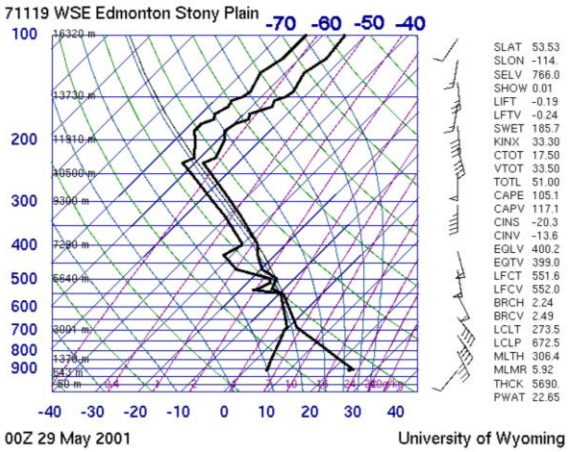

Figure 1: A classic inverted-V thermodynamic sounding associated with pyroCb formation (Edmonton, Alberta 0000 UTC, 29 May 2001, 150 km south of the Chisolm fire). The right-most black line shows air temperature as a function of height above the surface. The left-most black line shows the corresponding dew-point temperature. Reproduced from Fig. 4 of Rosenfeld et al. (2007).

METHODS: PLUME MODEL

Table 1: Plume model variables and constants

θ	Potential temperature (units K)
θ_{env}	Constant environment potential temperature (up to the condensation level)
θ_{fire}	Potential temperature of the fire/flames ($\theta_{fire} = \Delta\theta_f + \theta_{env}$)
θ_{pl}	Plume potential temperature
$\Delta\theta_f$	Fire potential temperature increment, per unit mass of combustion gas released
q	Specific humidity (units $kg\ kg^{-1}$, mass of water vapour to total mass of air)
q_{env}	Constant environment specific humidity (up to the condensation level)
q_{fire}	Fire specific humidity (includes moisture from the air consumed in combustion)
q_{pl}	Plume specific humidity
Δq_f	Fire moisture increment per unit mass of combustion gas released (includes evaporation of fuel moisture and moisture produced from the chemistry of combustion)
α	Plume dilution factor. Ranges from 1 (100% dilute = environment value) to 0 (pure combustion gas)
β	Plume buoyancy factor. Ranges from 0 (plume 100% dilute) to $\gamma - 1$. (Useful range $0 \rightarrow \sim 10^{-1}$.)
γ	Fire temperature multiplication factor to express θ_{fire} as a multiple of θ_{env}.
φ	Ratio of fire moisture to potential temperature increments (units $kg\ kg^{-1}\ K^{-1}$).

The fire plume is a mixture of hot combustion gases and entrained air from the immediate environment. This mixture could vary considerably throughout the plume and with time. The plume model focuses on hypothetical plume parcels (termed "plume elements") that begin as pure combustion gas and become increasingly diluted with time due to entrainment of environment air. The spatial and temporal plume mixture variability is represented in the model by an ensemble of plume elements. The plumes develop in a well-mixed (homogeneous) atmospheric boundary layer of constant potential temperature (θ_{env}) and constant specific humidity (q_{env}). The condensation level (CL, which is the saturation point on a thermodynamic diagram) for each plume element occurs within this well-mixed layer. While this latter condition is necessary to maintain model simplicity, the condition is unrealistic for CLs that are more elevated than the environment lifting condensation level (ELCL), because by definition the homogeneous boundary layer must be super-saturated in the cooler air above the ELCL. We demonstrate below that realistic CLs occur close to the ELCL, and that this unrealistic condition has no impact on the conclusions. For simplicity the thermodynamics of plume condensation, which begins at the CL, is not considered (i.e., the plume model begins at the fire and ends where condensation is about to occur). However, useful information on plume behaviour can be determined from the plume element thermodynamic quantities (θ_{pl} and q_{pl}) at the CL, and diagnostic quantities derived from these variables.

θ_{pl} and q_{pl} for each homogeneous plume element are expressed as functions of θ_{env} and q_{env}, the fire thermodynamic quantities (θ_{fire} and q_{fire}), and the plume dilution fraction α,

$$\theta_{pl} = \alpha\theta_{env} + (1-\alpha)\theta_{fire} \quad 1.$$

$$q_{pl} = \alpha q_{env} + (1-\alpha)q_{fire}. \quad 2.$$

θ_{env} and q_{env} are specified for each scenario, and α is varied to represent a range of plume dilution amounts from pure combustion gases at $\alpha = 0$ to pure environmental air at $\alpha = 1$ (i.e., infinitesimal quantities of combustion gases). These parameters and other variables introduced below are listed and described in Table 1.

The potential temperature of combustion gas, θ_{fire}, can be expressed as a multiplier (γ) of the environment potential temperature, $\theta_{fire} = \gamma\theta_{env}$. Assuming θ_{env}~$300\ K$, γ ranges from $2 \rightarrow 5$ representing flame temperature estimates from forest fires (e.g., Wotton et al. 2012) of 600 K (flame tips) to 1500 K (flame base)[1]. The fire produces increments of θ and q per unit mass of combustion gas (Luderer et al. 2009, hereafter LTA09), which we express respectively as, $\Delta\theta_f = (\gamma - 1)\theta_{env}$ and $\Delta q_f = \varphi\Delta\theta_f$. Here, φ, the ratio of the two increments, is a specified quantity. Δq_f incorporates the moisture of combustion and the evaporation of fuel moisture. Moisture from the air consumed in combustion is considered separately, such that $q_{fire} = \Delta q_f + 0.86 q_{env}$, with the latter term taking into account the 6 to 1 air to fuel mass ratio of combustion (e.g., Ward 2001).

An iterative process is used to calculate the CL based on estimates of the CL pressure (P_{CL}). The CL temperature is calculated from θ_{pl} and P_{CL}, which is used to calculate the saturation vapour pressure at P_{CL}. If this saturation vapour pressure is less than (greater than) the actual vapour pressure the plume must be saturated (unsaturated) at P_{CL} and the process is repeated at a lower (higher) level until the plume CL is approached to the nearest 1 hPa.

A number of diagnostic equations have been developed to illustrate plume characteristics. Each can be expressed as a function of a buoyancy-like parameter (e.g., Smith et al. 2005, Eq. 3),

$$\beta = \left(\theta_{pl} - \theta_{env}\right)/\theta_{env} = (1-\alpha)(\gamma - 1), \quad 3.$$

which reduces the experimental parameter space by replacing α and γ with β.

[1] Wotton et al. (2012) observed flame temperature ranges from about 600 to 1400 K in experimental forest fires. We chose an upper temperature of 1500 K to extend the parameter space to include potentially higher temperatures that might occur in very large and intense wild fires. This value matches observed temperatures for methane fires (*Smith et al. 1992)*.

RESULTS

Two well-mixed boundary layer profiles are considered, one warm (Fig. 2a) and the other cold (Fig. 2b,). The first has $\theta_{env} = 303\,K$, $q_{env} = 5{\times}10^{-3} kg\,kg^{-1}$, 19% relative humidity, and an elevated ELCL about 3 km above the surface. The second has $\theta_{env} = 271\,K$, $q_{env} = 2{\times}10^{-3} kg\,kg^{-1}$, 61% relative humidity, and a relatively low ELCL height (representing the Flatanger fire in Norway, January 2014, which destroyed 140 houses). The LCL is located at the apex of the θ_{env} and q_{env} curves.

SATURATION POINT CURVES

Fig. 2 includes SP curves for the hottest fire ($\gamma = 5$) in the warm environment (Fig. 2a) and the coolest fire ($\gamma = 2$) in the cold environment (Fig. 2b), and each with the two values of fire moisture to potential temperature increment ratios that represent LTA09's driest ($\varphi = 3{\times}10^{-5} kg\,kg^{-1}K^{-1}$, red) and wettest ($\varphi = 15{\times}10^{-5} kg\,kg^{-1}K^{-1}$, blue) realistic fires. Each SP curve represents the position of the plume element condensation level corresponding to α varying from 1 (100% dilution, lower left) to 0 (pure combustion gas, upper right) for the specified environment conditions, and the fire parameters, φ and γ. For example, the dots on the SP curves represent the apex of plume temperature and moisture traces for a plume element consisting of 95% environment air and 5% combustion gas.

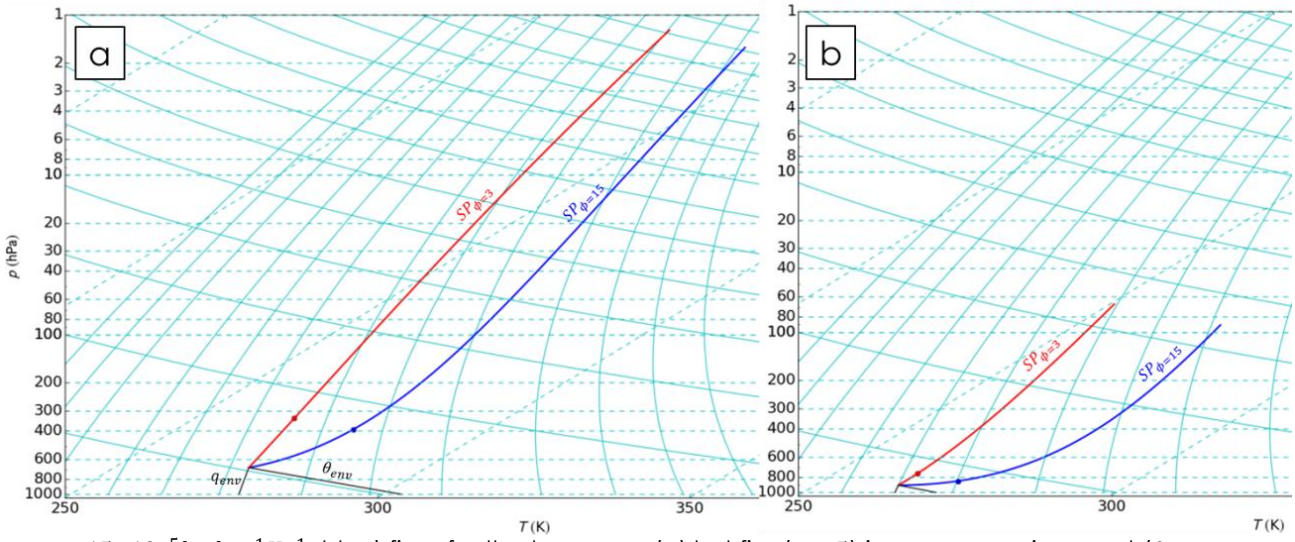

Figure 2: Saturation point curves for the dry ($\varphi = 3{\times}10^{-5} kg\,kg^{-1}K^{-1}$, red) and moist ($\varphi = 15{\times}10^{-5} kg\,kg^{-1}K^{-1}$, blue) fires, for the two cases (a) hot fire ($\gamma = 5$) in a warm environment ($\theta_{env} = 303\,K$), and (b) cool fire ($\gamma = 2$) in a cold environment ($\theta_{env} = 271\,K$), on a skewT-logp diagram. The 95% dilution points are indicated by dots. The environment LCL is located at the apex of the grey lines of constant θ_{env} and q_{env}. The pale blue lines are lines of constant pressure (dashed, horizontal), temperature (dashed, diagonal), potential temperature (solid, shallow gradient) and specific humidity (solid, steep gradient).

Of the parameter space investigated, the two most extreme cases are included in Fig. 2: hottest and driest fire in the warm environment (red curve in Fig. 2a), and coolest and moistest fire in the cold environment (blue curve in Fig. 2b). 100% dilution coincides with the ELCL, and zero dilution (at the upper right end of the coloured curves) shows exceptionally high CLs. These are ~1.5 hPa (> 40 km, Fig. 2a) and ~90 hPa (> 20 km, Fig. 2b).

Fig. 2a shows that for pyroCu/Cb to form in the lower troposphere (e.g., below 500 hPa) in the warm environment, significant dilution is necessary (e.g., > 95 %). The actual dilution amounts corresponding to the four SP curves (from left to right in Fig. 2) at 500 hPa, exceed, 99, 97, 85 and 75 % respectively (not shown). Furthermore, Large-Eddy Model simulations (LEM, Thurston et al. 2016) suggest typical dilution amounts in condensing plume elements are likely to be 99% or greater. It follows that substantial amounts of dilution must occur in typical pyroCu/Cb plumes (that form in warm/hot environments).

This result appears to be at odds with statements that suggest pyroCb formation requires plume cores that have experienced minimal (Taylor et al. 1973), or *zero* dilution/entrainment (e.g., "significant core of air unaltered by entrainment", Potter 2015; "a lack of entrainment to the convection column", Finney and McAllister 2011). The inconsistency arises from the fact that most plumes do not condense because they lose buoyancy after becoming too diluted. It follows that a somewhat less diluted plume or plume core is required for pyroCu/Cb formation (e.g., McRae et al. 2015). The plume model provides some quantification on how much less diluted condensing plumes need to be, and suggests that the amount is at the opposite end of the spectrum (large dilution) than that speculated in the aforementioned studies (small or zero dilution).

From Eq. 3 it can be seen that a plume element from a hot fire (γ) with moderate dilution (α) could have the same buoyancy (β) as a plume element from cooler fire with less dilution. This overlapping parameter space produces overlapping SP curves (i.e., varying γ only changes the length of the SP curve). Thus, all conclusions based on the position of the SP curve on thermodynamic diagrams are insensitive to the fire temperature. Hereafter, we discuss plume element buoyancy represented by the parameter β instead of fire temperature and plume element dilution. We conclude from Fig. 2 that for pyroCu/Cb to form in the lower troposphere, $\beta \leq O(10^{-1})$. Typical condensation level values of β in the LEM simulations are one to two orders of magnitude smaller than this (not shown).

Because β at condensation (β_{SP}) is small, the origin and gradient of the SP curves provide useful information about the height at which a plume element will condense, and thus the potential for pyroCu/Cb formation. The origin ($\beta_{SP} = 0$) coincides with the ELCL, which provides a first order estimate of the plume element condensation level. The difference between the actual plume element condensation height and the ELCL is of second-order importance (for small β_{SP}) which can be estimated from the product of β_{SP} and the SP curve gradient. Thus for a given β_{SP}, steep SP curves (e.g., dry fires) correspond to greater condensation heights than flatter SP curves (e.g., moister fires).

Fortunately, the most important factor for estimating plume condensation heights (the ELCL) does not require any information about the fire. The secondary factor is dependent on φ and β_{SP}. To determine β_{SP}, we expect detailed knowledge would be required of how plume buoyancy is affected by fire size, distribution and intensity, and how the atmosphere (e.g., wind and thermodynamic stability) affect the entrainment rate (plume dilution), and thus the distribution of β with height. One might also expect detailed knowledge of the fire and fuels would be required to determine φ. However, within the assumptions of the simple theoretical plume model (i.e., plume moisture and potential temperature are diluted at the same rate), φ remains constant

throughout the plume element (and is independent of β), which means it can be estimated from a single plume element measurement,

$$\varphi \cong \frac{q_{pl}-q_{env}}{\theta_{pl}-\theta_{env}}. \qquad 4.$$

In reality φ is likely to vary with time (and perhaps spatially), as the fire burns through a variety of fuels, but as long as the measurement is taken above the flaming zone (where additional radiative heat losses are relatively small) the measured plume element should maintain a constant φ throughout its ascent through a well-mixed boundary layer (constant θ_{env} and q_{env}). Multiple observations would produce a range of φ values, with a corresponding cluster of SP curves that represent the SP curve variability for the overall plume. Thus, in practice it should be possible to produce thermodynamic diagrams with the ELCL and a cluster of SP curves plotted, similar to Fig. 2, from observations at the fire ground, provided a representative sample of q_{pl} and θ_{pl} measurements can be made.

PLUME TEMPERATURE TRACES

The SP curves provide insight into the height at which a plume element might condense for a given environment (θ_{env}, q_{env}), fire properties (φ) and plume buoyancy (β), but they do not tell us anything about specific plumes. In Fig. 3 temperature and moisture traces from two LEM plume simulations (reported in Thurston et al. 2016) are plotted on thermodynamic diagrams with SP curves included. An extra SP curve has been added representing φ from one of Potter's (2005) fireCAPE thought experiments (green curve), which LTA09 argued was unrealistically moist.

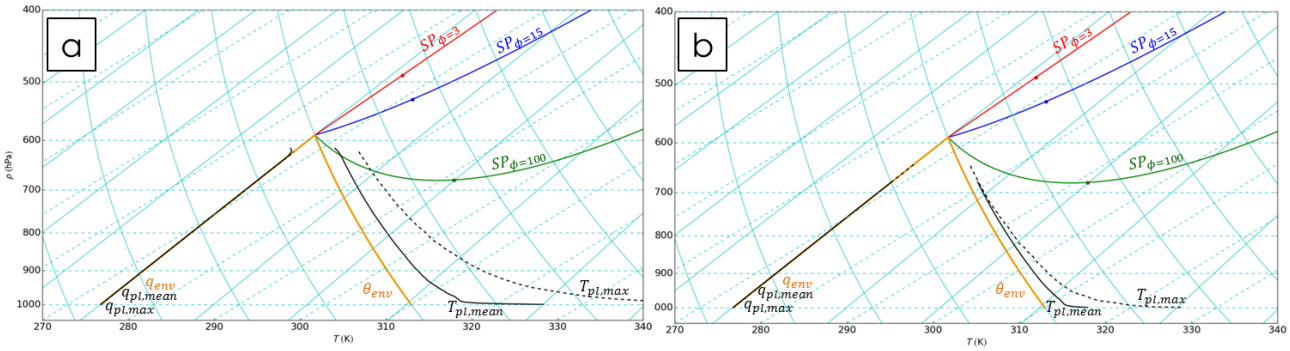

Figure 3: As in Fig. 2 but with mean (solid) and maximum (dashed) plume temperature and moisture traces in a hot and dry (θ_{env} = 310 K and $q_{env} = 4\times10^{-3} kg\ kg^{-1}$), zero wind environment from LEM simulations with a constant circular surface heat flux (Q)of 250 m radius. Saturation point curves for the dry (red, $\varphi = 3\times10^{-5} kg\ kg^{-1}K^{-1}$) moist (blue, $\varphi = 15\times10^{-5} kg\ kg^{-1}K^{-1}$) fires and an extremely moist fire (green, $\varphi = 100\times10^{-5}\ kg\ kg^{-1}K^{-1}$) are included. (a) hot fire ($Q = 30\ kWm^{-2}$) (b) cool fire ($Q = 5\ kWm^{-2}$).

As the LEM plume air ascends and approaches the ELCL it begins to entrain warm and dry environment air from above the boundary layer, which is a process that cannot be incorporated in our theoretical model. Thus, we discount the plume traces higher than about 620 hPa, and instead extrapolate them to the SP curves. Additionally, in order to make a clear distinction between plume and environment air, only plume elements that are at least 1 K warmer than the environment were included in the plume-average temperature trace. In reality

the plumes are expected to contain a mix of air parcels of temperature varying from the environment temperature (recently entrained parcels) up to the maximum temperature indicated by the dotted lines (least diluted plume elements).

For the hot fire (Fig. 3a) the mix of plume element temperatures would be expected to have a range of condensation heights extending from the ELCL to where the extrapolated dashed line meets the SP curve corresponding to the fire's φ value. The corresponding buoyancies range from $\beta_{SP} = 0 \rightarrow \beta_{SP,max}$ ($\beta_{SP,max} = 0.14$), with the plume element mean, $\beta_{SP,mean} = 0.04$. This simulation produced deep pyroCb with rain and evaporatively cooled downdrafts. Whereas the plume dilution was generally too great for condensation to occur in the cool fire simulation (Fig. 3b) as it mostly lost buoyancy near 650 hPa before intersecting any of the SP curves. A few parcels of buoyant air did occasionally reach the condensation level, producing short-lived puffs of shallow cloud.

WHAT CAN WE LEARN FROM THESE DIAGRAMS?

There is a surprising amount of information about conditions that support pyroCu/Cb development and plume behavior that can be gleaned from Figs 2 and 3.

- The positive gradients of the SP curves corresponding to the realistic range of fire moisture to potential temperature increment ratios (red and blue) demonstrate that buoyant plume elements condense at levels higher than the ELCL (consistent with LTA09 and Lareau and Clements 2016).
- An exception is for very moist fires (e.g., green SP curves in Fig. 3) and/or very dry environments (e.g., Fig. 2b) where the SP curve may have a negative gradient, in which case some buoyant elements might condense at levels lower than the ELCL (e.g., the Potter 2005 fireCAPE thought experiment). This is more likely to occur in cold and dry (small q) environments.
- Buoyant elements from moister fires will condense at lower levels than for drier fires.
- There is a broad range of temperatures and hence buoyancy within plumes, that decrease with height (due to dilution from entrainment, Fig. 3).
- Plumes with non-trivial buoyancy near their condensation level (e.g., Fig. 3a), contain plume elements with a range of buoyancy from zero to a maximum value corresponding to the least dilute plume element, with a corresponding range of condensation heights. These condensation heights are determined by the intersection of the plume element temperature trace and the relevant SP curve.

- Plumes that produce pyroCb (e.g., Fig. 3a) have non-trivial buoyancy near the condensation level, suggesting the fireCAPE[2] concept may be useful for pyroCb forecasting.
- The same LEM heat sources in environments with lower ELCLs (e.g., that might occur with the passage of a cold front or sea breeze) might produce very much more energetic pyroCb. At 900 hPa the hot fire β_{mean} and β_{max} are about three times greater than at 600 hPa, and the cool fire β_{mean} and β_{max} values at 900 hPa are very similar to the hot fire values at 600 hPa.

More insight will be described in a journal article (in preparation), based on a mathematical exploration of the model parameters. This journal article describes, among other things, how the environment affects the SP curves, what values of plume buoyancy are important for pyroCu/Cb activity, and the sensitivity of fireCAPE to plume buoyancy.

[2] FireCAPE is essentially a measure of the energy available for plume convection that takes into account the heat released from plume moisture condensation. It is analogous to the Convective Available Potential Energy (CAPE) used for predicting atmospheric moist convection.

SUMMARY

PyroCb can produce dangerous fire behaviour, through changes in fire rate of spread and direction, increased spotting, and additional ignitions from lightning strikes. Unfortunately, pyroCb is difficult to predict and not well understood.

In this paper we have introduced a simple theoretical model that provides useful insight into the conditions that influence plume condensation heights, the thermodynamic composition of fire plumes, and the relative sensitivity of environmental conditions to fire properties that have an influence on pyroCu/Cb formation and behaviour. Some of the more general results are summarized here:

- Substantial dilution (> 95%) is required for pyroCu/Cb cloud elements to condense in the lower troposphere for typical forest fire conditions. However, too much dilution and the plume may lose buoyancy before ascending high enough for condensation to occur.
- The environment lifting condensation level (ELCL) provides a good first order estimate of the plume condensation height.
- Typical forest fires that produce pyroCu/Cb will have buoyant plume elements that condense at elevations higher than the ELCL, because the additional heat provided by the fire contributes to raising the condensation level more than the additional moisture contributes to lowering the condensation level.
- PyroCu/Cb formation and behaviour is relatively insensitive to the amount of heat and moisture produced by the fire, but could be very sensitive to environment changes, such as might be experienced with the arrival of a cold front or sea-breeze that lowers substantially the ELCL due to the arrival of cooler and moister air.

REFERENCES

Cunningham, P. and M. J. Reeder, 2009: Severe convective storms initiated by intense wildfires: Numerical simulations of pyro-convection and pyro-tornadogenesis. *Geophys. Res. Lett.*, **36**, L12812, doi:10/1029/2009GLO39262.

Finney, M. A. and S. S. McAllister, 2011: A review of fire interactions and mass fires. *J. Combustion*, Article ID 548328, 14 pages. doi:10.1155/548328.

Fromm, M. D., A. Tupper, D. Rosenfeld, R. Servranckx and R. McRae, 2006: Violent pyro-convective storm devastates Australia's capital and pollutes the stratosphere. *Geophys. Res. Lett.*, **33**, L05815, doi:10.1029/2005FL025161.

Fromm, M. D., D. T. Lindsey, R. Servranckx, G. Yue, T. Trickl, R. Sica, P. Doucet and S. Godin-Beekman, 2010: The untold story of pyrocumulonimbus. *Bull. Amer. Met. Soc.*, 1193—1209

Fromm, M. D.,R. H. D. McRae, J. J. Sharples and G. P. Kablick III, 2012: Pyrocumulonimbus pair in Wollemi and Blue Mountains National parks, 22 November 2006. *Aus. Met. Ocean J.*, **62**, 117—126.

Goens, D. W. and P. L. Andrews, 1998: Weather and fire behavior factors related to the 1990 Dude Fire near Payson, Arizona. In: Proceedings: 2nd symposium on fire and forest meteorology. Boston, MA: American Meteorological Society: 153-158.

Johnson, R. H., R. S. Schumacher, J. H. Ruppert Jr., D. T. Lindsey, J. E. Ruthford and L. Kriederman, 2014: The role of convective outflow in the Waldo Canyon fire. *Mon. Wea. Rev.*, **142**, 3061—3080.

Koo, E., P. J. Pagni, D. R. Weise and J. P. Woycheese, 2010: Firebrands and spotting ignition in large-scale fires. *Int. J. Wild. Fire*, **19**, 818—843.

Lareau, N. P. and C. B. Clements, 2016: Environmental controls on pyrocumulus and pyrocumulonimbus initiation and development. *Atmos. Chem. Phys.*, **16**, 4005—4022. doi:10.5194/acp-16-4005-2016.

Luderer, G., J. Trentmann and M. O. Andreae, 2009: A new look at the role of fire released moisture on the dynamics of atmospheric pyro-convection. *Int. J. Wild. Fire*, **18**, 554—562.

McRae, R. H. D., Sharples, J. J., and Fromm, M.: Linking local wildfire dynamics to pyroCb development, Nat. Hazards Earth Syst. Sci., 15, 417-428, https://doi.org/10.5194/nhess-15-417-2015, 2015.

Peace, M., L. McCaw, B. Santos , J.D. Kepert, N. Burrows, and R.J.B. Fawcett, 2017: Meteorological drivers of extreme behaviour during the Waroona bushfire, Western Australia, January 2016. Submitted to *J. SH. Earth System Science.*

Peterson, D. A., E. J. Hyer, J. R. Campbell, M. D. Fromm, J. W. Hair, C. F. Butler and M. A. Fenn, 2015: The 2013 Rim Fire: Implications for predicting extreme fire spread, pyroconvection, and smoke emissions. *Bull. Amer. Met. Soc.*, 229—247. doi:10.1175/BAMS-D-14-00060.1.

Peterson, D. A., E. J. Hyer, J. R. Campbell, J. E. Solbrig and M. D. Fromm, 2017: A conceptual model for development of intense pyrocumulonimbus in western North America. *Mon. Wea. Rev.*, **145**, 2235–2255, https://doi.org/10.1175/MWR-D-16-0232.1

Potter, B. E., 2005: The role of released moisture in the atmospheric dynamics associated with wildland fires. *Int. J. Wild. Fire*, **14**, 77—84.

Rosenfeld, D., M. D. Fromm, J. Trentmann, G. Luderer, M. O. Andreae and R. Servanckx, 2007: The Chisolm firestorm: observed microstructure, precipitation and lightning activity of a pyro-cumulonimbus. *Atmos. Chem. Phys.*, **7**, 645—659.

Rudlosky, S. D and H. E. Fuelberg, 2011: Seasonal, Regional, and Storm-Scale Variability of Cloud-to-Ground Lightning Characteristics in Florida. *Mon. Wea. Rev.*, **139**, 1826–1843.

Smith, D, A, and G. Cox, 1992: Major chemical species in buoyant turbulent diffusion flames. *Combustion and Flame*, **91**, 226—238.

Smith, R, K, M. T. Montgomery and H. Zhu, 2005: Buoyancy in tropical cyclones and other rapidly rotating atmospheric vortices. *Dyn. Atm. and Oceans.*, **40**, 189—208.

Taylor, R. J., S. T. Evans, N. K. King, E. T. Stephens, D. R. Packham and R. G. Vines, 1973: Convective activity above a large-scale bushfire. *J. Applied Meteor.*, **12**, 1144—1150.

Thurston, W., K. J. Tory, R. J. B. Fawcett and J. D. Kepert, 2016: Large-eddy simulations of pyro-convection and its sensitivity to moisture, *5th International Fire Behaviour and Fuels Conference proceedings.* 6pp.

Tory, K. J. and W. Thurston, 2015: Pyrocumulonimbus: A literature review. *Bushfire and Natural Hazards CRC Report*, NO. 2015.067.

Tory, K. J., M. Peace and W. Thurston, 2016: Pyrocumulonimbus forecasting: Needs and issues. *Bushfire and Natural Hazards CRC Report, NO. 2016.239.*

Trentmann, J., G. Luderer, T. Winterrath, M. D. Fromm, R. Servranckx, M. Herzog, H.-F. Graf and M. O. Andrea, 2006: Modeling of biomass smoke injection into the lower stratosphere by a large forest fire (Part I): reference simulation. *Atmos. Chem. Phys.,* **6**, 5247—5260.

Ward, D, 2001: Combustion chemistry and smoke. In 'Forest Fires: Behavior and Ecological Effects'. (Eds EA Johnson, K Miyanishi) pp. 55–77. (Academic Press: San Diego, CA)